Lithium-Ion Battery State of Health Estimation Using Resampling-Based Data Simplification Deep Learning Techniques

Saran Techanok[1], **Nitikorn Junhuathon**[2], and **Keerati Chayakulkheeree**[1†], Non-members

ABSTRACT

Lithium-ion batteries (Li-ion) are widely used in various applications due to their high efficiency and reliability. However, as these batteries are continuously used, their performance gradually degrades over time, making accurate estimation of the State of Health (SOH) of increasing significance. One of the key challenges in SOH estimation lies in the nature of the measurement data collected during charge and discharge processes, which is typically time-series data with large volume and complexity. This results in increased computational load and reduced efficiency of the estimation models. To address this issue, this research proposes a data simplification method using a resampling technique aimed at identifying the optimal sampling level that maintains estimation accuracy while reducing computational cost. Four deep learning (DL) models are employed in this work: Long Short-Term Memory (LSTM), Bidirectional Long Short-Term Memory (Bi-LSTM), Attention-based LSTM (ATT-LSTM), and Gated Recurrent Unit (GRU). These models are trained and evaluated using public battery datasets that contain complete charge-discharge cycles. The proposed methods were tested with the Oxford Battery Dataset, and the experimental results demonstrate that the proposed approach achieves higher estimation accuracy while significantly reducing computation time.

Keywords: Lithium-ion battery, State of Health, Deep learning, Resampling

1. INTRODUCTION

Due to the severe growth of climate change caused by increasing greenhouse gas emissions, especially from the energy and transportation sectors, many countries around the world have begun taking action to curb these emissions. One major step is the Paris Agreement, which seeks to reduce the impact of climate change and encourages nations to set long-term carbon-reduction targets, thereby supporting a more environmentally sustainable future. Other significant frameworks, such as COP26 and the European Green Deal, likewise emphasize the transition to clean energy and a reduced reliance on fossil fuels. To meet these goals, renewable energy sources like solar and wind power have expanded rapidly, together with the development of energy storage systems (ESS) that store excess electricity for use during peak-demand periods. At the same time, electric vehicles (EVs) are becoming more popular as alternatives to traditional fuel-powered vehicles. Currently, lithium-ion batteries (Li-ion) are among the most popular battery types due to their high energy density, lightweight construction, and extended lifespan. Nevertheless, as they age, Li-ion batteries gradually degrade through chemical and physical changes, leading to diminished performance that can affect system safety and reliability. Consequently, monitoring and estimating a battery's state of health (SOH) is essential for predicting its remaining useful life, preventing unexpected failures, and enabling predictive maintenance strategies.

In recent years, the challenge of estimating the SOH of batteries has grown significantly, driven by the increasing adoption of renewable energy systems, EVs, and energy storage technologies. Batteries that are reliable and accurately monitored throughout their lifetime are crucial for these systems. As a result, SOH estimation has become an active area of research, especially approaches that learn directly from real-world battery data. Today, physics-based models for SOH estimation are becoming less reliable due to limitations in accuracy and flexibility. This has led to a growing shift toward using machine learning (ML) and artificial intelligence (AI) techniques to build data-driven models instead[1]. One basic model in the family of deep learning (DL) is the Artificial Neural Network (ANN), which has been applied in the estimation of various battery states such as the State of Charge (SOC), SOH, and remaining useful life (RUL) [2]. In [3], a multi-layer Long Short-Term Memory (LSTM) network combined with an attention mechanism was proposed, and then a backpropagation neural network was applied to integrate SOH estimations from different parts of the charging curve. Gaussian Process Regression (GPR) was used to reconstruct missing data, and an LSTM

Manuscript received on October 6, 2025; revised on December 15, 2025; accepted on December 29, 2025. This paper was recommended by Associate Editor Kampol Woradit.

[1]The authors are with School of Electrical Engineering, Institute of Engineering, Suranaree University of Technology, Nakhon Ratchasima, Thailand.

[2]The author is with Department of Electrical Engineering, Faculty of Engineering, Rajamangala University of Technology Thanyaburi, Pathum Thani, Thailand.

[†]Corresponding author: keerati.ch@sut.ac.th

Digital Object Identifier: 10.37936/ecti-eec.2026241.261516

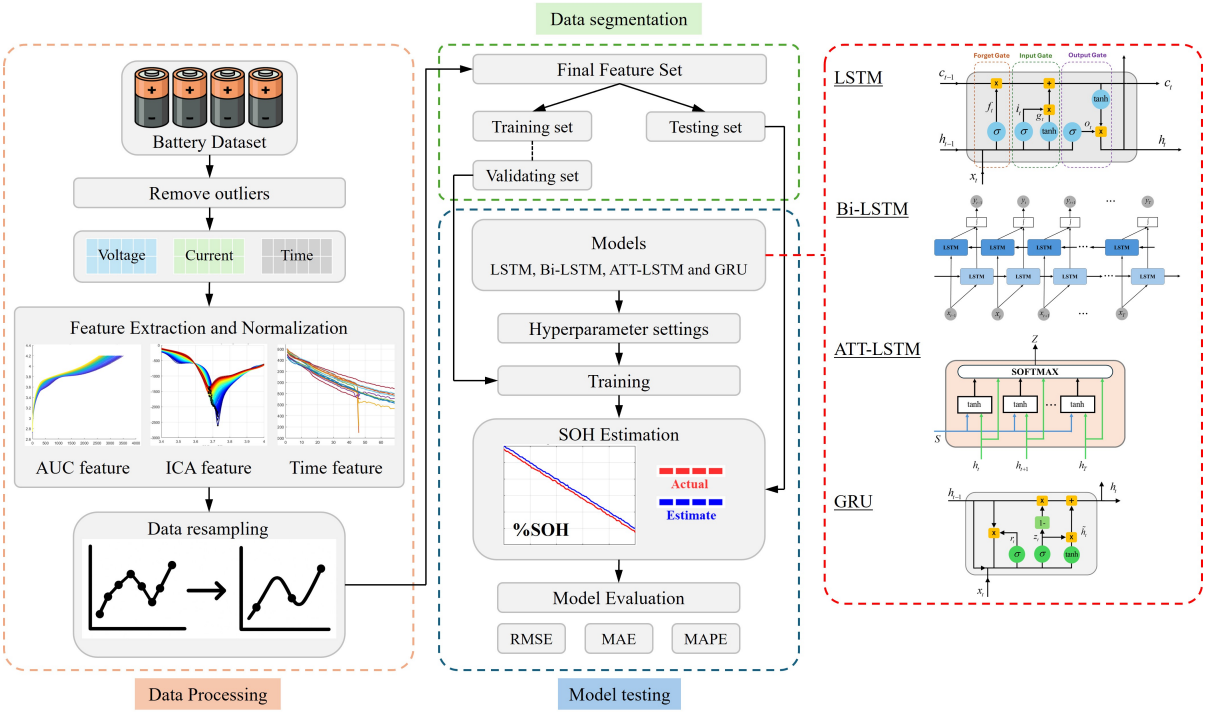

***Fig. 1**: Overall Framework of the Proposed Battery SOH Estimation.*

model was trained to estimate SOH from a section of the voltage sequence without relying on complex feature extraction [4]. A hybrid Gated Recurrent Unit (GRU)-CNN model was tested on NASA and Oxford datasets and showed a maximum estimation error of no more than 4.3% [5]. A separate evaluation comparing LSTM, GRU, 1D-CNN, and CNN-LSTM models found that 1D-CNN achieved the highest accuracy with the lowest variance [6]. Autoencoders were combined with LSTM to estimate SOH from voltage, current, and temperature data [7]. Controllable Deep Transfer Learning (CDTL) was used to estimate SOC in both short- and long-term periods during early-stage degradation, using two LSTM modules and a Multiple Domain Adaptation technique to transfer knowledge from batteries with extensive histories to new batteries with limited data [8]. The SOH-KLSTM model, which fuses LSTM with the Kolmogorov-Arnold Network (KAN), improved SOH estimation by capturing both time-based patterns and nonlinear degradation behavior [9]. The MC-CNN-TimesNet model was developed to estimate the SOH and RUL of Li-ion [10]. Apart from improving model architectures, feature extraction is also a key focus in many studies. Research [11] selected battery health features based on the area under constant current charging and discharging voltage curves across four types of Li-ion, showing a strong correlation between these extracted features and SOH. In [12], SOH was estimated using multiple features such as constant voltage discharge time, incremental capacity (IC), and differential thermal voltage (DTV) with a Bidirectional Long Short-Term Memory (Bi-LSTM) model incorporating an attention mechanism and achieved a minimum test RMSE of 0.162%. Moreover, feature extraction techniques that combine Differential Thermal Analysis (DTA) and Incremental Capacity Analysis (ICA) have been used to increase estimation accuracy [13]. The analysis of IC curve peaks combined with other variables has led to better SOH estimation results in [14] and [15]. A fusion-based method that integrates an OCV model and ICA with an ANN was presented in [16]. In [17], Fourier resampling was applied to process the signals, resulting in more uniform and denoised inputs. These processed signals were then used as model inputs, with IC features specifically selected to improve the accuracy of SOH estimation. The study in [18] introduced the MSHHO-DELM framework, which combines IC analysis with feature selection using Pearson correlation and Random Forest. It applies an improved Harris Hawks Optimization algorithm with multi-strategy mechanisms to avoid local optima during training. This method produced a lowest test RMSE of 0.32 on the Oxford dataset. In [19], nine data-driven approaches for Li-ion SOH estimation are compared. The method includes ICA and feature extraction, then uses a variety of machine learning algorithms to predict SOH. Two publicly available datasets are used to assess the models' processing time and estimation error. Results show that ML methods offer faster processing than experimental techniques, making them suitable for accelerating industrial battery testing.

Although research in battery SOH estimation has explored a wide range of model types and hybrid model developments aimed at reducing estimation error, another important perspective that can also improve

performance lies in enhancing the quality of input data before training. This includes reducing training time, simplifying the input structure, and minimizing computational complexity, which are crucial factors for enabling real-world deployment of SOH models. The overall framework of the proposed method utilized to address these challenges is illustrated in Fig. 1. Despite their importance, these aspects often remain underexplored in the existing literature. The related studies are summarized in Table 1. The table compares whether each study applied resampling techniques. For those that did, it considers whether the sampling intervals were defined with sufficient granularity to capture broader patterns and trends.

It also compares the input and output variables used in each study. This highlights a research gap in previous works regarding the comprehensive selection and analysis of resampling intervals. In summary, the main contributions of this analysis are:

- Applying a resampling technique to reduce the resolution of time-series data, making it more manageable for model training and computation.
- Utilizing input features based on ICA and area under the curve (AUC) extraction to enhance SOH estimation.
- Comparing four DL models: LSTM, Bi-LSTM, Attention-based LSTM (ATT-LSTM), and GRU to identify the most effective model for estimating SOH.

This article is organized into several sections. Section 2 presents the battery datasets used in this study. Section 3 explains the feature extraction process based on a data-driven approach. Section 4 describes the DL models selected for SOH estimation, including the techniques used for data handling. Section 5 presents the comparative performance of all four models across the different resampling intervals. Section 6 concludes the study.

2. BATTERY DATASETS

The Oxford Battery Degradation Dataset 1, containing aging data from eight 740 mAh Kokam SLPB533459H4 Li-ion pouch cells, was employed in this study. All tests were conducted in a thermal chamber maintained at a constant temperature of 40 °C. The cells underwent a constant-current–constant-voltage (CC–CV) charging process, followed by discharging, with a 1C charge/discharge test conducted every 100 drive cycles. The resulting data were used for analysis and visualization. Each test applied a constant current of 740 mA, with measurements recorded at a sampling rate of one second. The recorded parameters include time (t, seconds), voltage (v, volts), charge (q, mAh), and temperature (T, °C). Figure 2 shows the voltage and current profiles during the charging and discharging cycles. In this study, the data were trimmed to use only the voltage range between 2.7 V and 4.2 V: charging corresponds to the voltage rising from 2.7 V to 4.2 V,

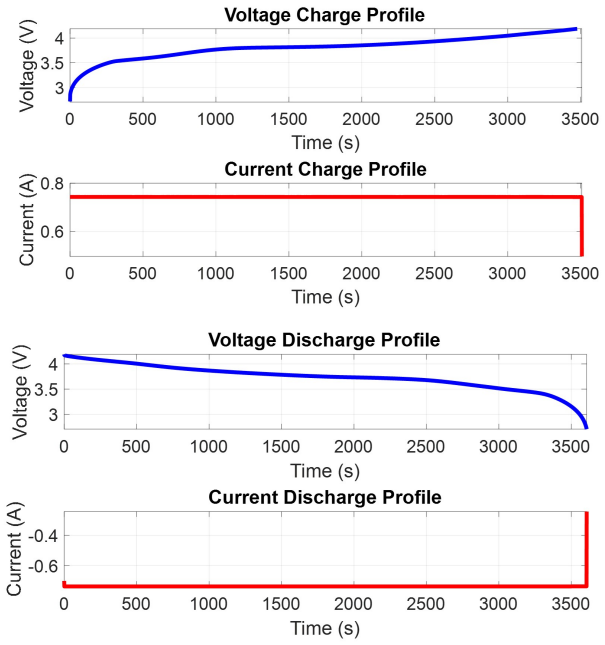

Fig. 2: Voltage and Current Profiles During Charging and Discharging cycles at a 1C rate.

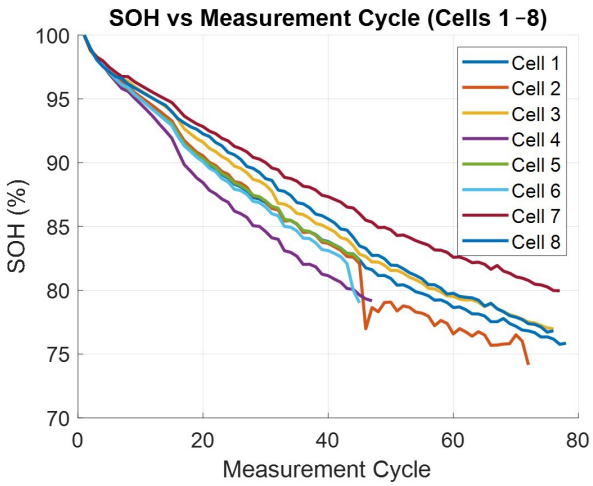

Fig. 3: SOH Degradation Curves of all 8 cells.

while discharging corresponds to the voltage decreasing from 4.2 V down to 2.7 V. These graphs provide an overview of the general battery behavior under the given test conditions. In Fig 3, the SOH of each cell was plotted as a function of the number of charge-discharge cycles. This visualization helps highlight the gradual decline in capacity and gives an overview of the aging characteristics under repeated cycling. The SOH is defined by the remaining capacity (C_{remain}) compared to the initial capacity ($C_{initial}$) [27], as shown in Eq. (1):

$$\%SOH = \frac{C_{remain}}{C_{initial}} \tag{1}$$

***Table 1**: Review of Related Literature.*

Ref.	Year	Resampling	Intervals Investigation	Algorithm	Input features and output
[14]	2020	-	-	Bi-LSTM	Input = [ICA], Output = SOH
[5]	2020	✓	-	GRU-CNN	Input = [Charging curves], Output = SOH
[7]	2021	-	-	Autoencoders- LSTM	Input = [V, I, T], Output = RUL
[20]	2021	✓	3 intervals	CNN, ULSAM, GRU	Input = [V, I, T], Output = SOC
[16]	2022	-	-	ANN	Input = [OCV, ICA], Output = SOH
[6]	2022	-	-	LSTM, GRU, 1D-CNN, CNN-LSTM	Input = [V, I, T], Output = SOH
[8]	2022	-	-	CDTL	Input = [V, I, T, V_{avg}], Output = SOH
[21]	2022	-	-	GPR	Input = [voltage curves], Output = SOH
[22]	2022	-	-	DL	Input/Output = Various (as reviewed)
[12]	2023	-	-	Bi-LSTM-AM	Input = [ICA, DTV], Output = SOH
[15]	2023	-	-	BP, PCR	Input = [ICA, PCA], Output = SOH
[23]	2023	-	-	LSTM, FNN	Input = [V, I, T], Output = SOH, RUL
[24]	2023	-	-	TCN-LSTM	Input = [V, I, T, t], Output = SOH, RUL
[11]	2023	-	-	GPR, LSTM, BP	Input = [voltage curve], Output = SOH
[25]	2023	-	-	LSTM	Input = [Capacity], Output = RUL
[4]	2023	✓	-	GPR, LSTM	Input = [ICA], Output = SOH
[3]	2023	-	-	Ensemble	Input = [Charging curves], Output = SOH
[13]	2024	-	-	GPR	Input = [ICA, DTA], Output = SOH
[17]	2024	✓	-	LSTM, DNN, GRU	Input = [ICA], Output = SOH
[26]	2024	✓	-	CNN-LSTM	Input = [V, T, capacity], Output = SOH
[1]	2024	-	-	ML and AI	Input/Output = Various (as reviewed)
[2]	2024	-	-	ANN, FNN, CNN	Input/Output = Various (as reviewed)
[19]	2024	-	-	9 data-driven techniques	Input = [ICA], Output = SOH
[18]	2025	-	-	MSHHO-DELM	Input = [ICA, V], Output = SOH
[27]	2025	-	-	LSTM	Input = [AUC_v, V, I, T], Output = SOH
[9]	2025	-	-	SOH-KLSTM	Input = [V, I, T, capacity], Output = SOH
[10]	2025	-	-	MC-CNN-TimesNet	Input = [Charging curves], Output = RUL
[28]	2025	-	-	Bagged-GPR	Input = [R, V], Output = SOH
Proposed Models		✓	9 intervals	LSTM, Bi-LSTM, ATT-LSTM, GRU	Input = [AUC, ICA], Output = SOH

3. FEATURE EXTRACTION

Extracting features that represent the battery's deterioration behavior over time is crucial for accurate SOH estimation. These characteristics are usually obtained from unprocessed data, including voltage and current readings, that are captured during charge-discharge cycles. Feature extraction highlights the most pertinent attributes for ML model training while assisting in reducing the dimensionality of the input. However, the raw data may contain recording errors or segments affected by electrical noise in some cells. Therefore, data cleaning and preprocessing are necessary before conducting analysis or extracting features.

3.1 Area under the curve

AUC is a metric used to measure the total magnitude of a variable over a period of time. In this study, the AUC is used to analyze the voltage and current patterns recorded during the battery's charging and discharging cycles. It is utilized as a feature to indicate how the battery uses energy and how this behavior changes over time. Because the AUC aggregates the overall signal instead of focusing on single points, it can give a clearer picture of the battery's behavior, even if there are small fluctuations or noise in the data. This makes it effective for monitoring gradual changes that occur as the battery degrades. The AUC is calculated using the trapezoidal integration method, as shown in the following Eq. (2):

$$AUC = \int_{t_0}^{t_n} x(t) = \sum_{i=1}^{n-1} \frac{\left(x_i + x_{i+1}\right)}{2} \cdot \left(t_{i+1} - t_i\right) \quad (2)$$

where x_t represents either the voltage or current at time t, and t_0 to $t_n$are the time intervals during the cycle. Figure 4 shows the voltage profiles during the discharging process for all cycles, plotted against time. This allows for a direct comparison of how the voltage curve changes over time as the battery ages. The AUC value represents the total voltage over each cycle, starting from the first

cycle through to the later ones. This information can be used to analyze the relationship between battery degradation and the SOH.

From the voltage profiles in Fig. 4, another feature can be extracted: the charging and discharging time duration (Time). This feature represents the accumulated time from the start of the cycle until the voltage (or current) reaches the specified cut-off endpoint. Degradation mechanisms cause the battery voltage to reach the cut-off threshold significantly faster, resulting in a continuous decrease in the total duration. This trend correlates strongly with the reduction in battery capacity.

Consequently, we utilized the time at which the voltage reaches the cut-off endpoint as one of the input variables, as it effectively reflects the battery's health status.

3.2 Incremental Capacity Analysis

ICA is a non-destructive analytical technique used to examine the electrochemical behavior of a battery during charging and discharging cycles. This method is based on the derivative of battery capacity (Q) with respect to voltage (V), expressed by Eq. (3):

$$ICA = dQ/dV \tag{3}$$

The resulting dQ/dV curve which translates raw voltage data into a representation of electrochemical activity, reveals distinct features that evolve as the battery ages. Specifically, the minimum point of the dQ/dV curve for each cycle serves as a key indicator of degradation. This feature is highly sensitive to internal changes, such as the loss of active material and lithium inventory. For this reason, ICA is widely regarded as an effective approach for generating reliable features to estimate the battery's SOH. However, a practical challenge arises from the fact that the raw dQ/dV curves often exhibit significant noise, which can interfere with accurate feature extraction. Therefore, to improve data quality, a Moving Average (MA) filter was applied for data smoothing. Figure 5 presents the resulting ICA curves after this filtering process. In this study, a filter window size of 400 was selected. This value was empirically chosen to effectively reduce noise while preserving the essential shape of the curve. This smoothing process is a crucial pre-processing step that ensures that the subsequent identification of key degradation features is both more reliable and robust.

Following the feature extraction process, all extracted features AUC, Charging and Discharging Time Duration, and ICA are normalized using the Min-Max Normalization method to rescale all feature values to a uniform range between 0 and 1. Preventing features with wider numerical ranges from controlling the model's learning process is the main goal of this normalization. Every feature will contribute more equally to the final estimation thanks to this standardization.

Furthermore, to quantitatively validate the relevance of the selected features, a correlation analysis was performed. The results are presented as a correlation matrix in Fig. 6.

This matrix illustrates the strength and direction of the linear relationship between each feature and the battery's SOH. A high correlation coefficient, whether positive or negative, indicates a strong relationship, confirming that the extracted features are indeed sensitive and reliable indicators of the battery's health degradation.

3.3 Data Resampling

Data resampling is a process of adjusting the structure or resolution of time-series data, with the goal of making the data more suitable for analysis or model training. In this study, the focus is placed on reducing the frequency of input data. The main objective is to simplify the data in order to reduce training time and computational cost, while still maintaining an acceptable level of accuracy in the estimation of battery SOH.

For the experiments, thirteen resampling intervals were considered: no resampling (None), and down-sampling by skipping data every 20, 40, 60, 80, 100, 120, 140, 160, 180, 200, 300, and 400 seconds. This design allows an evaluation of how reducing the amount of input data affects the model's performance, and whether prediction accuracy can still be preserved effectively. Ultimately, this experiment represents an important step in identifying the optimal balance between data volume and model performance.

3.4 Min-Max Normalization

Min-Max Normalization is a method of scaling data into a predefined range from 0 to 1, which helps address the issue of varying magnitudes across different features. This process is important for ensuring that input data remain proportionate and balanced, making them more suitable for model training. The general formula is defined in Eq. (4):

$$x' = \frac{x - x_{min}}{x_{max} - x_{min}} \tag{4}$$

where x represents the original data value x_{min} and are x_{max} the minimum and maximum values of the data, respectively, and x' is the normalized value. In this study, Min-Max Normalization was applied to the selected features, including ICA, AUC, and Time. By scaling all features into the same range, the model can better capture the underlying patterns of the data and improve the effectiveness of SOH estimation.

4. DEEP LEARNING MODELS

As previously discussed, various DL models are employed for battery SOH estimation. In this study, the resampled data are input into LSTM, Bi-LSTM, ATT-LSTM, and GRU models to compare their estimation performance. The following subsections provide a brief description of each model.

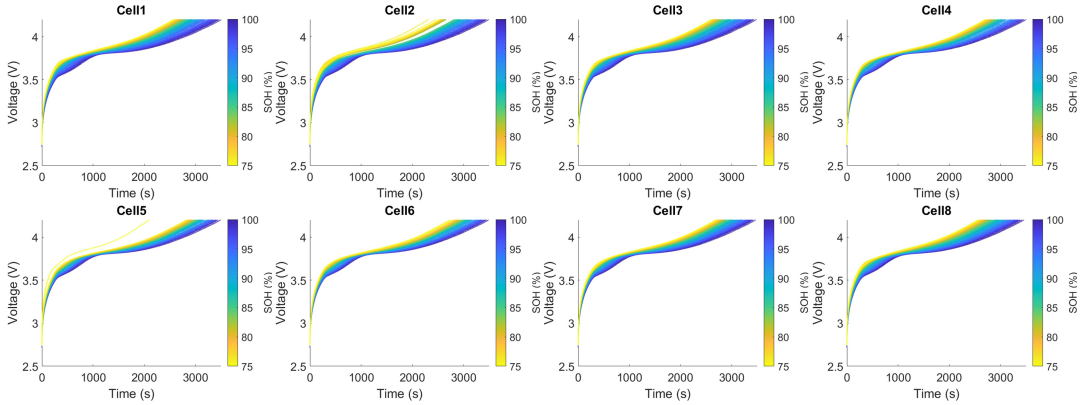

***Fig. 4**: Voltage Profiles are Used to Charge all the cycles.*

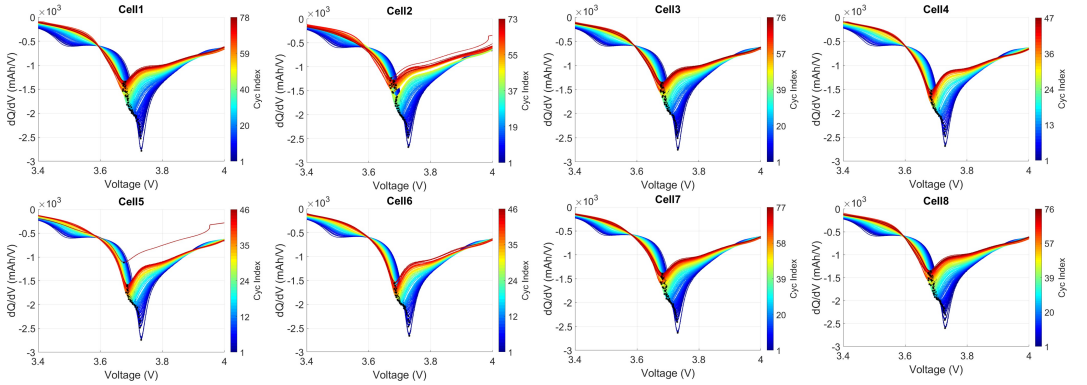

***Fig. 5**: ICA Curve all the cycles 8 cells.*

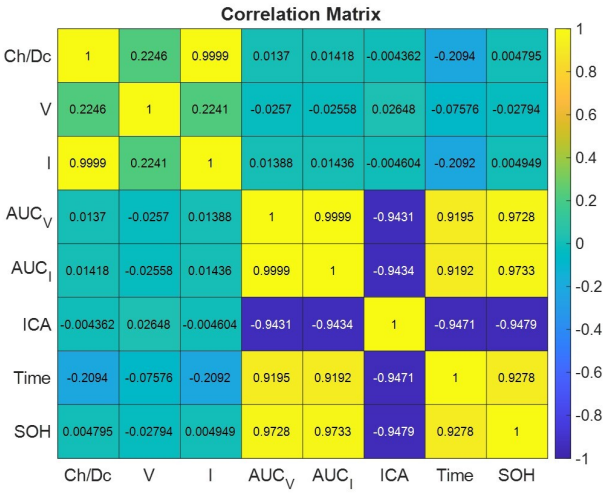

***Fig. 6**: The Correlation Matrix of all Parameters.*

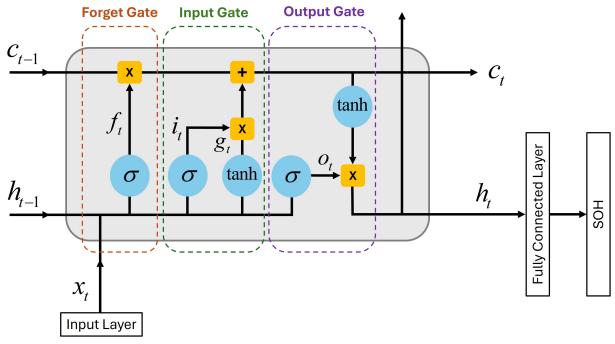

***Fig. 7**: The LSTM Network Architecture.*

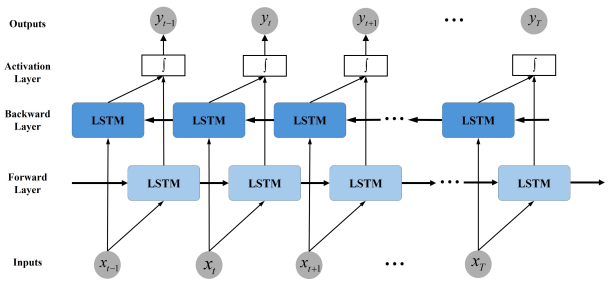

***Fig. 8**: The Bi-LSTM Network Architecture.*

4.1 Long Short-Term Memory

LSTM is a type of recurrent neural network (RNN) developed to address the problem of learning long-term dependencies in time-series data. Three main gates complement the memory cell that serves as the foundation of LSTM. The input gate regulates how new data is added to the memory cell, the output gate chooses what data is output at each time step, and

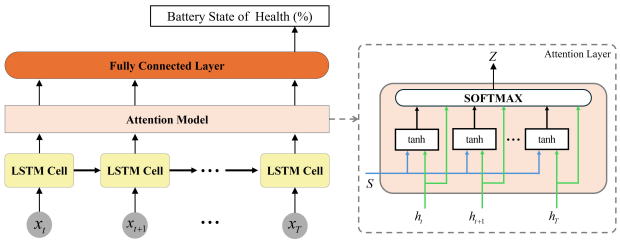

***Fig. 9**: The ATT-LSTM Network Architecture.*

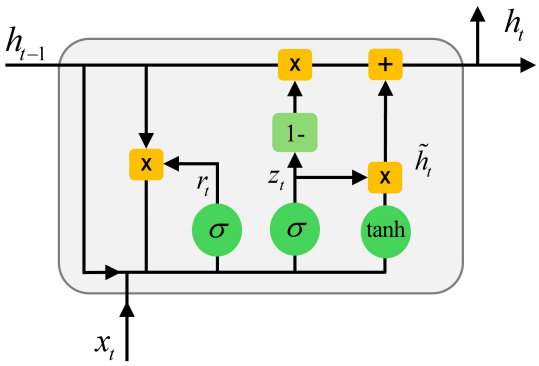

***Fig. 10**: The GRU Network Architecture.*

the forget gate chooses which data to discard. The memory cell is capable of storing important information for extended periods of time, as shown in Fig. 7. These mechanisms enable the model to retain important information, learn patterns in sequential data, and adapt to complex temporal dependencies effectively, additional information about LSTM can be found in [26].

4.2 Bidirectional Long Short-Term Memory

Bi-LSTM builds upon the conventional LSTM by simultaneously processing input sequences in both forward and backward directions, enabling the network to draw on contextual information from earlier and later time steps at once. This dual-directional design strengthens the model's ability to learn intricate temporal relationships. Although it maintains the memory cells and gate operations used in LSTM, its distinctive feature is merging the outputs from both directions to form a richer representation. Further information about Bi-LSTM is provided in [12], and the architecture of the model is illustrated in Fig. 8.

4.3 Attention-based LSTM

An attention mechanism is included into the memory cell of the ATT-LSTM, an enhanced variant of the conventional LSTM. As a result, rather than considering every time step identically, the model can concentrate on the most crucial portions of the input sequence. The attention mechanism creates a context vector by combining the hidden states of each time step with different weights according to their importance, as illustrated in Fig. 9. While keeping the memory cells and gate structure of a regular LSTM, ATT-LSTM emphasizes key time steps, helping the model capture complex relationships in the sequence and retain the most relevant information effectively. A detailed explanation of ATT-LSTM is provided in [12].

***Table 2**: Hyperparameter Settings.*

Parameter	Value
Optimizer	adam
Max Epochs	100
Mini-Batch Size	1024
Initial Learning Rate	0.01
Learning Rate Schedule	piecewise
Learning Rate Drop Factor	0.5
Learning Rate Drop Period	40
Shuffle	every-epoch
Validation Frequency	500

4.4 Gated Recurrent Unit

The GRU is a simplified version of recurrent neural networks aimed at capturing long-term dependencies in sequential data. In contrast to LSTM, it features a more straightforward structure with just two primary gates: the update gate, which controls the merging of new inputs with existing information, and the reset gate, which decides how much of the prior context should be abandoned. Unlike the LSTM, the GRU does not use a separate memory cell but instead incorporates the memory mechanism directly into its hidden state, resulting in fewer parameters, faster training, and an effective ability to model sequential patterns. For more detailed information on the GRU, readers are referred to [17]. The architecture of the GRU is presented in Fig. 10.

In this study, four models LSTM, Bi-LSTM, ATT-LSTM, and GRU were used for comparison. To ensure fairness and reliability of the results, the same hyperparameter settings were applied to all models. The selected values were chosen to balance accuracy and computational time. Using identical hyperparameters also allows the impact of resampling to be evaluated more clearly without being influenced by differences in model configurations. This approach ensures that the learning behavior and performance of each model can be assessed under the same conditions. The detailed hyperparameter settings are presented in Table 2.

Table 2 presents the hyperparameter settings that are applied consistently across all models. The only difference lies in the Output Mode. The ATT-LSTM model is configured to use the sequence mode, since the Attention Layer requires the complete sequence of outputs. In contrast, the LSTM, Bi-LSTM and GRU models use the last mode, which considers only the final output of the sequence for prediction.

4.5 Evaluation Metrics

To evaluate the performance of battery SOH estimation, three common metrics were selected: Root

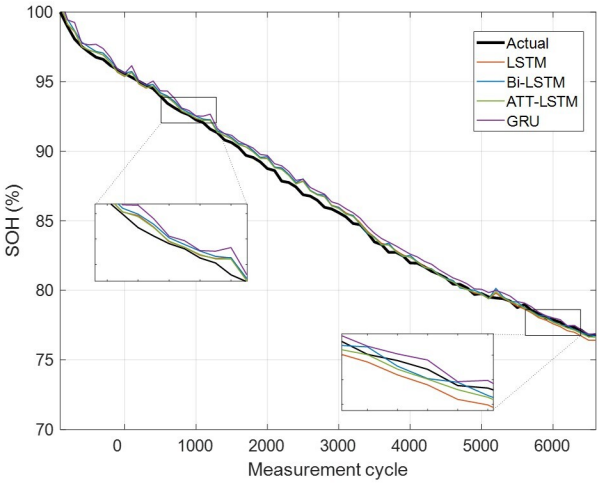

***Fig. 11**: SOH Estimation Results at the Best Interval.*

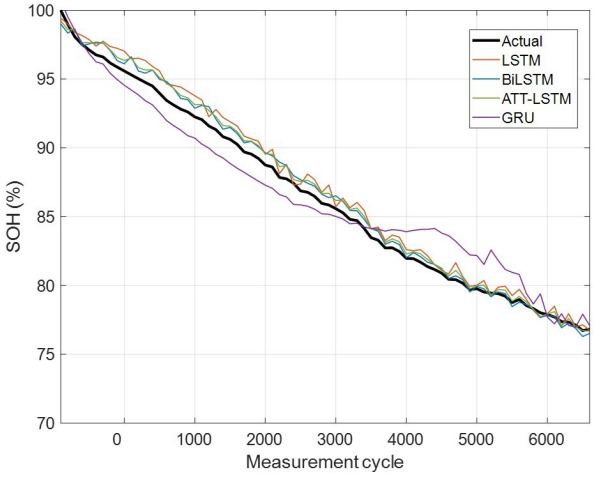

***Fig. 12**: Error Comparison at the Best Interval.*

Mean Square Error (RMSE), Mean Absolute Error (MAE), and Mean Absolute Percentage Error (MAPE). The first, RMSE, is frequently used to display, in terms of root mean square, the average difference between estimated and actual values. which is calculated as:

$$RMSE = \sqrt{\frac{1}{n}\sum_{i=1}^{n}\left(SOH\,(i) - SOH_e(i)\right)^2} \qquad (5)$$

where n is a number of cycles, SOH is actual capacity, SOH_e is estimated capacity. Next, MAE focuses on the overall error using absolute differences, which helps reduce the effect of extreme mistakes defined as:

$$MAE = \frac{1}{n}\sum_{i=1}^{n}\left|SOH\,(i) - SOH_e(i)\right| \qquad (6)$$

Finally, MAPE makes it simple to compare accuracy across several scales by expressing the error as a percentage. MAPE is defined as:

$$MAPE = \frac{1}{n}\sum_{i=1}^{n}\left|\frac{SOH\,(i) - SOH_e(i)}{SOH\,(i)}\right| \times 100\% \qquad (7)$$

5. COMPARATIVE ANALYSIS

In this section, a comparative analysis is presented by evaluating the effect of different resampling intervals. Thirteen cases are considered: None, 20, 40, 60, 80, 100, 120, 140, 160, 180, 200, 300, and 400 seconds, as described earlier. The objective is to identify the most suitable interval for accurate SOH estimation of Li-ion batteries. In addition, the performance of four DL models, LSTM, Bi-LSTM, ATT-LSTM, and GRU, is compared to determine which model can extract features most effectively from the data derived from AUC, ICA, and Time. In this study, to ensure that the data sets are non-overlapping and to reduce bias in the evaluation, the

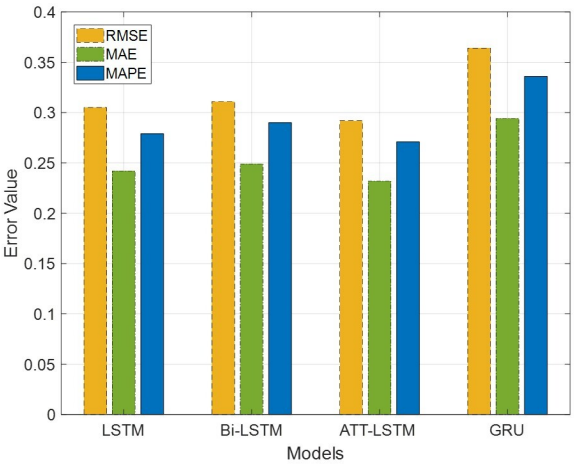

***Fig. 13**: SOH Estimation Results at the Worst Interval.*

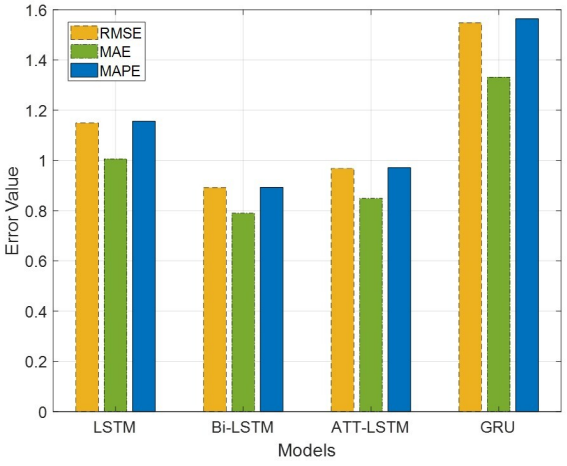

***Fig. 14**: Error Comparison at the Worst Interval.*

Oxford battery data was divided into three main sets. Cells 1–6 were used for training the models, allowing them to learn the degradation patterns of the batteries. Cell 7 was assigned as the validation set to fine-tune

***Table 3**: SOH Estimation Results.*

Resampling Interval	LSTM			Bi-LSTM			ATT-LSTM			GRU		
	RMSE	MAE	MAPE	RMSE	MAE	MAPE	RMSE	MAE	MAPE	RMSE	MAE	MAPE
None	0.922	0.722	0.810	0.631	0.523	0.596	0.705	0.585	0.669	1.548	1.331	1.564
20 s	0.760	0.609	0.684	0.816	0.667	0.747	0.781	0.592	0.658	0.676	0.400	0.445
40 s	0.483	0.364	0.420	0.558	0.427	0.478	0.545	0.452	0.534	0.457	0.362	0.433
60 s	0.406	0.332	0.385	0.456	0.382	0.450	0.362	0.286	0.339	0.413	0.328	0.373
80 s	0.388	0.340	0.299	0.387	0.311	0.367	0.327	0.256	0.294	0.407	0.317	0.363
100 s	0.305	0.242	0.279	0.311	0.249	0.290	0.292	0.232	0.271	0.364	0.294	0.336
120 s	0.324	0.257	0.296	0.332	0.254	0.289	0.311	0.239	0.271	0.377	0.308	0.350
140 s	0.383	0.314	0.360	0.333	0.263	0.299	0.340	0.270	0.305	0.396	0.325	0.369
160 s	0.401	0.325	0.368	0.334	0.258	0.292	0.357	0.278	0.313	0.432	0.349	0.396
180 s	0.470	0.389	0.440	0.347	0.272	0.308	0.349	0.278	0.316	0.481	0.394	0.447
200 s	0.527	0.446	0.503	0.359	0.287	0.326	0.363	0.279	0.313	0.520	0.448	0.508
300 s	0.783	0.694	0.795	0.621	0.527	0.591	0.621	0.527	0.593	0.747	0.669	0.760
400 s	1.149	1.006	1.156	0.892	0.790	0.893	0.968	0.849	0.971	1.145	0.999	1.152

***Table 4**: Execution Time of Each Model.*

Resampling Interval	Processing Time (seconds)			
	LSTM	Bi-LSTM	ATT-LSTM	GRU
None	14,056	17,071	15,891	13,403
20 s	447.44	556.63	848.22	403.20
40 s	217.60	261.42	382.18	205.79
60 s	160.95	184.59	264.02	139.29
80 s	105.93	139.20	228.70	103.12
100 s	84.09	115.34	169.12	85.65
120 s	70.88	97.72	131.52	72.78
140 s	58.68	82.53	106.82	59.77
160 s	51.83	66.61	93.07	51.50
180 s	48.37	64.98	96.74	51.05
200 s	44.85	57.15	84.37	45.14
300 s	30.09	40.14	57.09	30.80
400 s	23.57	28.96	41.05	23.43

model parameters and prevent overfitting. Cell 8 was set aside for testing, offering an objective evaluation of the model's capacity to calculate SOH from unknown data. By using this data partitioning technique, the outcomes will more precisely represent how well the model generalizes to new batteries.

The experimental results show that applying resampling initially leads to a steady reduction in error, indicating that selecting an appropriate resampling interval helps the models learn and capture the data relationships more effectively. This improves the accuracy of SOH estimation. However, when the resampling interval becomes too large, specifically greater than 100-second, the error starts to increase again. This trend is observed starting from 120-second, where the error gradually rises as the gap widens up to 400-second. This suggests that as the data becomes too coarse, the models lose important details, making it more difficult to capture meaningful patterns. This trend is observed across all four models. The best performance is achieved at the 100-second interval, where the MAPE for LSTM is 0.279, while the error values for Bi-LSTM, ATT-LSTM which is the best among all models, and GRU are 0.290, 0.271, and 0.336 respectively. These results are illustrated in Fig. 11, which shows the SOH estimation of all four models at their best-performing interval. On the other hand, the worst results are observed at the 400-second interval for LSTM, Bi-LSTM, and ATT-LSTM, with error values of 1.156, 0.893, and 0.971 respectively, while the worst case for GRU occurs when no resampling is applied, with an error value of 1.564. These results are shown in Fig. 12, which presents the SOH estimation of the four models under the least favorable conditions. In addition, bar charts are provided to compare the error values at the best interval, which are shown in Fig. 13, and at the worst interval, which are shown in Fig. 14 across all models, highlighting the performance differences more clearly. A complete summary of these results is provided in Table 3. In addition to evaluating SOH estimation using the three previously mentioned metrics, the models were also assessed based on Processing Time, which refers to the time each model requires to train and generate the SOH estimation results. Analyzing processing time provides insight into not only the accuracy of each model but also which models are faster or slower in computation. The experimental results presented in Table 4 compare the processing times of each model across different resampling intervals, showing that processing time generally decreases as the resampling interval increases. When comparing the models at their best-performing resampling interval of 100 seconds, the LSTM model demonstrated the fastest performance, requiring only 84.09 seconds. It was followed closely by the GRU at 85.65 seconds, while the Bi-LSTM and ATT-LSTM models required longer processing times of 115.34 and 169.12 seconds, respectively. This indicates that while all models benefit from resampling, the standard LSTM architecture offers the greatest computational speed among the evaluated models.

Regarding overall performance, the ATT-LSTM model achieved the highest accuracy with a MAPE of 0.271, yet it consumed the most processing time (169.12 seconds). In contrast, the LSTM model required only 84.09 seconds, approximately half the duration of the ATT-LSTM, while achieving a very similar accuracy with a MAPE of 0.279. When comparing the LSTM model's performance between the raw data (None) and the 100-second resam-

pling interval, the estimation error decreased by 65.56%, while the processing time was significantly reduced by 99.40%. Therefore, considering the trade-off between high estimation accuracy and computational efficiency, the LSTM is identified as the most suitable model for real-world applications where resource constraints are a concern.

6. CONCLUSION

This research focused on the estimation of the SOH of Li-ion by investigating the impact of resampling on the performance of DL models. Several models, including LSTM, Bi-LSTM, GRU, and ATT-LSTM, were evaluated under different resampling intervals to analyze both estimation accuracy and processing time. The results showed that selecting an appropriate resampling interval can reduce data complexity and suppress noise, which improves the learning efficiency of the models. This leads to lower estimation errors and significantly shorter processing times. However, when the resampling interval becomes too large, the models may lose important details in the data, making it harder to capture the relationships needed for accurate SOH estimation.

In practice, resampling offers potential for real-world applications such as battery health monitoring in ESS and EVs. By reducing the amount of data while maintaining accuracy, it allows faster processing and more efficient use of computational resources. This makes it possible to apply these models in systems that require reliable and near real-time SOH estimation.

ACKNOWLEDGEMENT

This work is fully supported by Suranaree University of Technology.

REFERENCES

[1] A. Dineva, "Evaluation of Advances in Battery Health Prediction for Electric Vehicles from Traditional Linear Filters to Latest Machine Learning Approaches," *Batteries*, vol. 10, no. 10, p. 356, Oct. 2024.

[2] A. G. Olabi, A. A. Abdelghafar, B. Soudan, A. H. Alami, C. Semeraro, M. Al Radi, M. Al-Murisi, and M. A. Abdelkareem, "Artificial Neural Network Driven Prognosis and Estimation of Lithium-Ion Battery States: Current Insights and Future Perspectives," *Ain Shams Engineering Journal*, vol. 15, no. 2, p. 102429, Feb. 2024.

[3] L. Zhang, J. Zhang, T. Gao, L. Lyu, L. Wang, W. Shi, L. Jiang, and G. Cai, "Improved LSTM Based State of Health Estimation Using Random Segments of the Charging Curves for Lithium-Ion Batteries," *Journal of Energy Storage*, vol. 74, p. 109370, Dec. 2023.

[4] X. Xiong, Y. Wang, K. Li, and Z. Chen, "State of Health Estimation for Lithium-Ion Batteries Using Gaussian Process Regression-Based Data Reconstruction Method During Random Charging Process," *Journal of Energy Storage*, vol. 72, p. 108390, Nov. 2023.

[5] Y. Fan, F. Xiao, C. Li, G. Yang, and X. Tang, "A Novel Deep Learning Framework for State of Health Estimation of Lithium-Ion Battery," *Journal of Energy Storage*, vol. 32, p. 101741, Dec. 2020.

[6] A. Aliberti, F. Boni, A. Perol, M. Zampolli, R. J. P. Jaboeuf, P. Tosco, E. Macii, and E. Patti, "Comparative Analysis of Neural Networks Techniques for Lithium-Ion Battery SOH Estimation," in *2022 IEEE 46th Annual Computers, Software, and Applications Conference (COMPSAC)*, Los Alamitos, CA, USA, 2022, pp. 1355-1361.

[7] P. Audin, I. Jorge, T. Mesbahi, A. Samet, F. D. B. D. Beuvron, and R. Boné, "Auto-Encoder LSTM for Li-Ion SOH Prediction: A Comparative Study on Various Benchmark Datasets," in *2021 20th IEEE International Conference on Machine Learning and Applications (ICMLA)*, Pasadena, CA, USA, 2021, pp. 1529-1536.

[8] I. Oyewole, A. Chehade, and Y. Kim, "A Controllable Deep Transfer Learning Network with Multiple Domain Adaptation for Battery State-of-Charge Estimation," *Applied Energy*, vol. 312, p. 118726, May 2022.

[9] I. Jarraya, S. Ben Atitallah, F. Alahmed, M. Abdelkader, M. Driss, F. Abdelhadi, and A. Koubaa, "SOH-KLSTM: A Hybrid Kolmogorov-Arnold Network and LSTM Model for Enhanced Lithium-Ion Battery Health Monitoring," *Journal of Energy Storage*, vol. 122, p. 116541, Jun. 2025.

[10] Y. Li, X. Qin, M. Chai, H. Wu, F. Zhang, F. Jiang, and C. Wen, "SOH Evaluation and RUL Estimation of Lithium-Ion Batteries Based on MC-CNN-TimesNet Model," *Reliability Engineering & System Safety*, vol. 261, p. 111125, Sep. 2025.

[11] J. Wu, Z. Liu, Y. Zhang, D. Lei, B. Zhang, and W. Cao, "Data-Driven State of Health Estimation for Lithium-Ion Battery Based on Voltage Variation Curves," *Journal of Energy Storage*, vol. 73, p. 109191, Dec. 2023.

[12] B. Zou, M. Xiong, H. Wang, W. Ding, P. Jiang, W. Hua, Y. Zhang, L. Zhang, W. Wang, and R. Tan, "A Deep Learning Approach for State-of-Health Estimation of Lithium-Ion Batteries Based on a Multi-Feature and Attention Mechanism Collaboration," *Batteries*, vol. 9, no. 6, p. 329, Jun. 2023.

[13] D. Stephens, Q. Zhou, H. Hofmann, and J. Sun, "Integrated Incremental Capacity Analysis and Differential Thermal Analysis for Improved Robustness in Li-Ion Battery State of Health Estimation," in *2024 IEEE Conference on Control Technology and Applications (CCTA)*, Newcastle upon Tyne, UK, 2024, pp. 729-734.

[14] H. Sun, J. Sun, K. Zhao, L. Wang, and K. Wang, "Data-Driven ICA-Bi-LSTM-Combined Lithium

Battery SOH Estimation," *Mathematical Problems in Engineering*, vol. 2022, p. 9645892, Mar. 2022.

[15] Z. Zou, Y. Li, X. Liu, Z. Zhang, B. Duan, and C. Zhang, "Fast Estimation of State of Health for Retired Lithium-Ion Batteries Based on Principal Component Regression," in *2023 7th CAA International Conference on Vehicular Control and Intelligence (CVCI)*, Changsha, China, 2023, pp. 1-6.

[16] X. Bian, Z. Wei, W. Li, J. Pou, D. U. Sauer, and L. Liu, "State-of-Health Estimation of Lithium-Ion Batteries by Fusing an Open Circuit Voltage Model and Incremental Capacity Analysis," *IEEE Transactions on Power Electronics*, vol. 37, no. 2, pp. 2226-2236, Feb. 2022.

[17] K. D. Rao, N. V. Anand, T. K. S. Pandraju, F. Alsaif, and T. S. Ustun, "Optimally Tuned Gated Recurrent Unit Neural Network-Based State of Health Estimation Scheme for Lithium Ion Batteries," *IEEE Access*, vol. 12, pp. 58597-58607, 2024.

[18] Z. Wei, Y. Li, X. Sun, W. Liu, C. Liu, and H. Lu, "SOH Estimation of Lithium-Ion Batteries Based on Multi-Feature Extraction and Improved DLEM," *Journal of Energy Storage*, vol. 120, p. 116460, May 2025.

[19] P. Eleftheriadis, M. Gangi, S. Leva, A. V. Rey, E. Groppo, and L. Grande, "Comparative Study of Machine Learning Techniques for the State of Health Estimation of Li-Ion Batteries," *Electric Power Systems Research*, vol. 235, p. 110889, Oct. 2024.

[20] Q. Gong, P. Wang, Z. Cheng, and J. Zhang, "A Method for Estimating State of Charge of Lithium-Ion Batteries Based on Deep Learning," *Journal of The Electrochemical Society*, vol. 168, no. 11, p. 110532, Nov. 2021.

[21] Z. Wang, G. Feng, X. Sun, D. Zhen, F. Gu, and A. D. Ball, "Feature Extraction from Charging Profiles for State of Health Estimation of Lithium-Ion Battery," *Journal of Physics: Conference Series*, vol. 2184, no. 1, p. 012024, Jan. 2022.

[22] M. S. Hossain Lipu, S. Ansari, M. S. Miah, S. T. Meraj, K. Hasan, A. S. M. Shihavuddin, M. A. Hannan, K. M. Muttaqi, and A. Hussain, "Deep Learning Enabled State of Charge, State of Health and Remaining Useful Life Estimation for Smart Battery Management System: Methods, Implementations, Issues and Prospects," *Journal of Energy Storage*, vol. 55, p. 105752, Nov. 2022.

[23] C. Nguyen Van and D. T. Quang, "Estimation of SOH and Internal Resistances of Lithium Ion Battery Based on LSTM Network," *International Journal of Electrochemical Science*, vol. 18, no. 6, p. 100166, Jun. 2023.

[24] C. Li, X. Han, Q. Zhang, M. Li, Z. Rao, W. Liao, X. Liu, X. Liu, and G. Li, "State-of-Health and Remaining-Useful-Life Estimations of Lithium-Ion Battery Based on Temporal Convolutional Network-Long Short-Term Memory," *Journal of Energy Storage*, vol. 74, p. 109498, Dec. 2023.

[25] L. Zhang, T. Ji, S. Yu, and G. Liu, "Accurate Prediction Approach of SOH for Lithium-Ion Batteries Based on LSTM Method," *Energy Reports*, vol. 9, pp. 3206-3214, Nov. 2023.

[26] V. Safavi, N. Bazmohammadi, J. C. Vasquez, and J. M. Guerrero, "Battery State-of-Health Estimation: A Step Towards Battery Digital Twins," *Electronics*, vol. 13, no. 2, p. 384, Jan. 2024.

[27] S. Techanok, N. Junhuathon, and K. Chayakulkheeree, "A Comparative Study on Feature Extraction for Battery State of Health Estimation: Evaluating the Role of Open Circuit Voltage in LSTM Model," in *2025 13th International Electrical Engineering Congress (iEECON)*, Phuket, Thailand, 2025, pp. 1-6.

[28] W. Ma, S. Ha, G. Pozzato, A. Saatchi, N. Aliahmad, K. Littau, and S. Onori, "Engineering Testing Protocols for Machine Learning-Based SOH Estimation in Lithium Metal Batteries," *Journal of The Electrochemical Society*, vol. 171, no. 12, p. 120531, Dec. 2024.

Saran Techanok received his B.Eng in EE (First Class Honors) from Suranaree University of Technology (SUT), Thailand, in 2024. He is now enrolled in M.Eng in EE at School of EE, Institute of Engineering, SUT. His research area is on power system and AI applications in power systems.

Nitikorn Junhuathon was born in Nakhon Ratchasima in Thailand, on February 23, 1995. He received his B. Eng., M. Eng., and Ph.D. In Electrical Engineering from Suranaree University of Technology (SUT), Thailand, in 2017, 2019 and 2023, respectively. He is currently a lecturer at Department of Electrical Engineering, Faculty of Engineering, Raja Mangala University of Technology Thanyaburi (RMUTT), Thailand. His research interests are machine learning and optimization technique for power forecasting, electric vehicle application, and related fields.

Keerati Chayakulkheeree received his B. Eng. in Electrical Engineering from King Mongkut's Institute of Technology Ladkrabang (KMITL) in 1995, and M. Eng. and D. Eng. degrees in Electric Power System Management from the Asian Institute of Technology (AIT), Thailand, in 1999 and 2004, respectively. He is an Associate Professor at the School of Electrical Engineering, Institute of Engineering, Suranaree University of Technology (SUT), Nakhon Ratchasima, Thailand. His research interests include power system optimization, AI applications in power systems, smart grid technology, power system protection, distributed energy resources, electricity market restructuring, renewable energy integration, and carbon emissions in the power sector.